21. S.-T. Wu, Q.-H. Wang, M. D. Kempe, and J. A. Kornfield, "Perdeuterated cyanobiphenyl liquid crystals for infrared applications," J. Appl. Phys. **92**(12), 7146–7148 (2002).
22. Y. Chen, H. Xianyu, J. Sun, P. Kula, R. Dabrowski, S. Tripathi, R. J. Twieg, and S.-T. Wu, "Low absorption liquid crystals for mid-wave infrared applications," Opt. Express **19**(11), 10843–10848 (2011).
23. F. Peng, Y. Chen, S.-T. Wu, S. Tripathi, and R. J. Twieg, "Low loss liquid crystals for infrared applications," Liq. Cryst. **41**(11), 1545–1552 (2014).
24. B. Mistry, *A Handbook of Spectroscopic Data Chemistry: UV, IR, PMR, CNMR and Mass Spectroscopy* (Oxford Book Company, Jaipur, India, 2009).
25. S.-T. Wu, D. Coates, and E. Bartmann, "Physical properties of chlorinated liquid crystals," Liq. Cryst. **10**(5), 635–646 (1991).
26. M. Schadt, "Field-effect liquid-crystal displays and liquid-crystal materials: key technologies of the 1990s," Displays **13**(1), 11–34 (1992).
27. M. Hird, "Fluorinated liquid crystals - properties and applications," Chem. Soc. Rev. **36**(12), 2070–2095 (2007).
28. Y. Chen, Z. Luo, F. Peng, and S.-T. Wu, "Fringe-field switching with a negative dielectric anisotropy liquid crystal," J. Disp. Technol. **9**(2), 74–77 (2013).
29. I. Haller, "Thermodynamic and static properties of liquid crystals," Prog. Solid State Chem. **10**, 103–118 (1975).
30. I. H. Malitson, "Refractive properties of barium fluoride," JOSA **54**(5), 628–630 (1964).
31. J. Li, S.-T. Wu, S. Brugioni, R. Meucci, and S. Faetti, "Infrared refractive indices of liquid crystals," J. Appl. Phys. **97**(7), 073501 (2005).
32. S.-T. Wu, "Infrared markers for determining the order parameters of uniaxial liquid crystals," Appl. Opt. **26**(16), 3434–3440 (1987).
33. H. Kneppe, F. Schneider, and N. K. Sharma, "Rotational viscosity γ1 of nematic liquid crystals," J. Chem. Phys. **77**(6), 3203–3208 (1982).
34. I.-C. Khoo and S.-T. Wu, *Optics and Nonlinear Optics of Liquid Crystals* (World Scientific, 1993).
35. M. Zhang, S. Fang, A. A. Zakhidov, S. B. Lee, A. E. Aliev, C. D. Williams, K. R. Atkinson, and R. H. Baughman, "Strong, transparent, multifunctional, carbon nanotube sheets," Science **309**(5738), 1215–1219 (2005).
36. D. S. Hecht, L. Hu, and G. Irvin, "Emerging transparent electrodes based on thin films of carbon nanotubes, graphene, and metallic nanostructures," Adv. Mater. **23**(13), 1482–1513 (2011).

1. Introduction

Liquid crystals (LCs) are an amazing class of soft materials which have been widely used in the visible [1, 2], infrared (IR) [3], millimeter wave [4], and terahertz [5, 6] spectral regions. Both amplitude modulation (such as displays [7]) and phase modulation (e.g., tunable prism for laser beam steering [8] and adaptive lenses [9]) have been investigated extensively. Different applications may emphasize different LC properties, e.g. birefringence (Δn), dielectric anisotropy ($\Delta\varepsilon$), rotational viscosity (γ_1), resistivity, absorption, nematic range, UV stability, and molecular alignment. For intensity modulation, twisted nematic [10], in-plane switching [11], and vertical alignment [12] have been used in display devices. But for phase modulation, 2π phase modulo is generally required so that homogeneous alignment with a positive $\Delta\varepsilon$ LC is preferred [13]. The phase change (δ) of a homogeneous cell is governed by the cell gap (d) and wavelength (λ) as:

$$\delta = 2\pi d\Delta n / \lambda. \quad (1)$$

From Eq. (1), the condition $d\Delta n = \lambda$ is required to obtain a 2π phase change. In the visible region, say λ = 0.5 μm, this condition can be easily satisfied but in the mid-wave infrared (MWIR, λ = 3-5 μm) region, say λ = 5 μm, the required $d\Delta n$ is ~10X larger than that at λ = 0.5 μm. Moreover, as the wavelength increases, Δn decreases and then gradually saturates [14]. Thus, a fairly large cell gap is needed, which leads to slow response time. Let us take E7 as an example. It has a Δn≈0.2 at λ = 5 μm and so to achieve a 2π phase change the required cell gap is 25 μm, which in turn leads to a slow response time (~1s). To achieve submillisecond response time, a polymer network liquid crystal (PNLC) has been explored at λ = 1.06 μm and 1.55 μm [15, 16]. In a PNLC, the phase change is determined by $d\Delta n$ (Eq. (1), but the response time is governed by the average domain size [17]. Thus, the phase change is decoupled from the response time. The small domain size helps to suppress light scattering and shorten response time, but the trade-off is increased operating voltage [18].

#226796 - $15.00 USD Received 13 Nov 2014; revised 22 Dec 2014; accepted 22 Dec 2014; published 8 Jan 2015

In order to increase Δn while retaining good UV stability, we can extend the conjugation length by adding phenyl rings to the core. However, the use of too many phenyl rings would result in some undesirable properties: 1) the melting point is too high and its solubility in a LC host is very limited [6]; 2) its viscosity increases dramatically, and 3) its birefringence gradually saturates once there are more than three phenyl rings. Therefore, terphenyls (three rings) could be an optimal conjugation length [19]. One common approach to lower high melting points of liquid crystals is to formulate eutectic mixtures.

For IR applications, another important factor needs to be considered, which is absorption originating from vibrations of molecular bonds and functional groups. To reduce absorption loss, several approaches have been investigated: 1) Shifting the absorption bands outside the spectral region of interest by deuteration [20, 21], fluorination [22], or chlorination [23]. 2) Reducing the cell gap by using a high Δn LC mixture. 3) Choosing a proper polar group. Isothiocyanate (NCS), cyano (CN), fluorine (F) and chlorine (Cl) are commonly used polar groups. Although NCS provides a large Δn and $\Delta \varepsilon$ while keeping a modest viscosity, its characteristic vibration absorption band is strong and broad in the 4.5-5.2 μm spectral range [24]. Thus, from an absorption viewpoint, NCS compounds are not desirable for MWIR applications. On the other hand, CN has a strong dipole moment and it is compatible to monomers for making PNLC devices. Although its absorption peak at ~4.45μm is strong, its bandwidth is relatively narrow. Therefore, high transmittance in the off-resonance region can still be achieved. Fluoro and chloro polar groups offer high resistivity, good UV stability, and modest dipole moment [25–27] and they are widely used in thin-film transistor LC displays [28].

In this paper, we report a terphenyl LC mixture, which shows high birefringence (Δn = 0.34 at λ = 514nm and Δn = ~0.253 at λ = 4μm), high transmittance (T>98%) in the MWIR region, and broad nematic range. Using this mixture, we fabricated three PNLC devices with different polymer concentrations and studied how domain sizes affect the operation voltage and response time. We believe this first PNLC result is promising for MWIR applications, especially its response time is about 100X faster than that of the nematic LC host.

2. Experiment and results

Table 1 lists two series of terphenyl compounds we prepared. Compounds 1 through 4 are fluorinated cyano-terphenyls. The terphenyl core extends the conjugation and increases birefringence. The fluoro substitutions help to lower the melting temperatures. The phase transition temperatures were measured by Differential Scanning Calorimetry (DSC). As shown in Table 1, these cyano compounds exhibit a fairly high melting point. To lower the melting point, we formulated a eutectic mixture (called M1) from these four compounds. The melting point of M1 is still higher than room temperature (RT = 22°C). Compounds 5 and 6 are chlorinated terphenyls, which show a fairly low absorption and modest birefringence at MWIR [23]. We formulated a binary mixture (M2) using compound 5 and compound 6. In order to further lower the melting point while maintaining high Δn, we mixed 35 wt% M2 with 65 wt% M1, and designated the final mixture as M3. Remarkably, the melting point of M3 drops to below –40°C (limited by our DSC) and its clearing point is 149.7°C. Thus, M3 shows an extraordinarily broad nematic range surrounding room temperature.

In order to characterize the physical properties of M3, we prepared a homogeneous cell with a cell gap d≈5μm. The ITO (indium tin oxide) glass substrates were over-coated with a thin polyimide (PI) layer rubbed in anti-parallel directions to create a 3° pretilt angle and strong anchoring energy. The cell was filled with M3 by capillary flow at 70°C and mounted in a Linkam LTS 350 Large Area Heating/Freezing Stage controlled by TMS94 Temperature Programmer. Birefringence was determined by measuring the voltage-dependent transmittance (VT) of the homogeneous cell sandwiched between two crossed linear polarizers. To achieve maximum transmittance, the LC director was oriented at 45° with respect to the transmission axis of polarizer. A tunable Argon-ion laser (λ = 457, 488, and

#226796 - $15.00 USD Received 13 Nov 2014; revised 22 Dec 2014; accepted 22 Dec 2014; published 8 Jan 2015

514nm), He-Ne laser (λ = 633nm) and a semiconductor laser (λ = 1550nm) were used as light sources. A 1 kHz square-wave AC signal was applied to the LC cell and the transmitted light was measured by a photodiode and recorded by a LabVIEW data acquisition system (DAQ, PCI6110).

Table 1. Chemical structures and phase transition temperatures of the seven terphenyl compounds employed. T_{mp} represents melting point and T_c clearing point.

Compound #	Chemical structure	T_{mp} (°C)	T_c (°C)
1	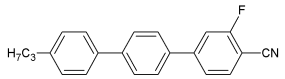	109	199
2	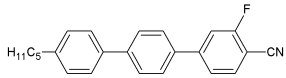	86	183
3	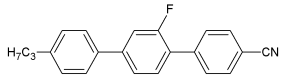	91	208
4	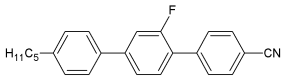	93	191
5	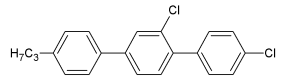	95	68
6	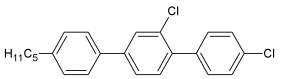	71	65

2.1 Birefringence

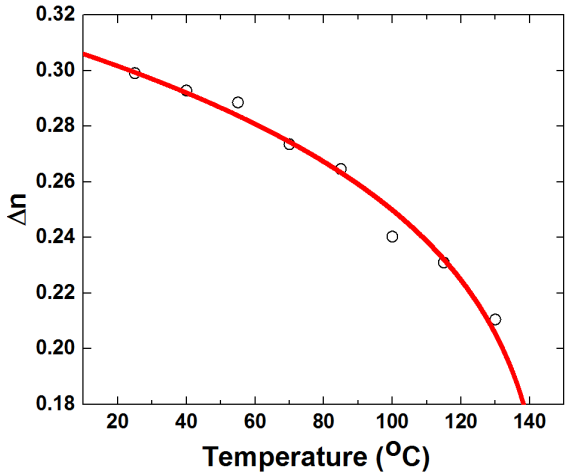

Fig. 1. Temperature dependent birefringence of M3 at λ = 633nm: the circles are measured data and the red line is a fitting curve with Eq. (2).

We can obtain the birefringence at a given temperature from Eq. (1) using the VT curve and the wavelength and cell gap. We measured the temperature dependence of the Δn of M3 from

#226796 - $15.00 USD Received 13 Nov 2014; revised 22 Dec 2014; accepted 22 Dec 2014; published 8 Jan 2015

25°C to 130°C and the results for λ = 633nm are plotted in Fig. 1. Circles in Fig. 1 are experimental data and solid line is a fit with Haller's semi-empirical equation [29]:

$$\Delta n = \Delta n_0 (1 - T/T_c)^{\beta}, \quad (2)$$

where Δn_0 stands for the extrapolated birefringence at T = 0K and β is a material constant. Through fitting, we found Δn_0 = 0.38 and β = 0.19. The adjusted R^2 = 0.9768.

Figure 2 shows the birefringence dispersion of M3. The red line is the fitting curve given by the single-band birefringence dispersion equation where G is a proportionality constant and λ^* is the mean resonance wavelength [14].

$$\Delta n = G \frac{\lambda^2 \lambda^{*2}}{\lambda^2 - \lambda^{*2}}, \quad (3)$$

Through fitting, we found G = 3.78 μm^{-2} and λ^* = 0.258 μm. The adjusted R^2 = 0.9996. Based on these parameters, the birefringence at any wavelength can be calculated. According to Fig. 2, the birefringence decreases to a plateau and its value is about 15%~20% lower in the MWIR region. For M3, its birefringence remains relatively high (Δn = ~0.253) at λ = 4μm. Based on Δn = ~0.253, we found that the required cell gap for $\delta = 2\pi$ at λ = 4μm is about 16μm. High Δn enables a thin cell gap to be used for achieving 2π phase change, which in turn improves transmittance and response time in the MWIR region.

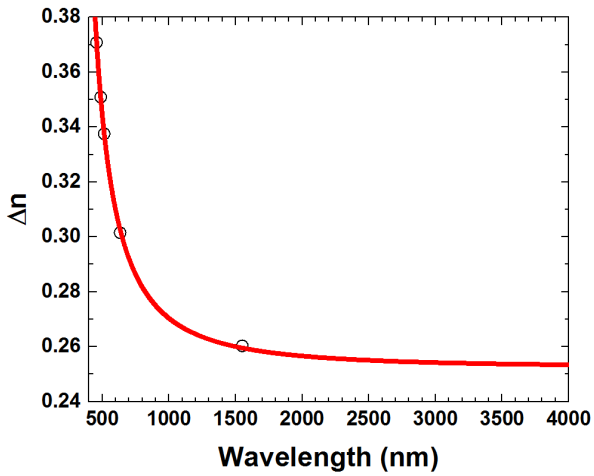

Fig. 2. Birefringence dispersion of M3 at room temperature: circles are measured data and solid line is fitting with Eq. (3).

2.2 MWIR transmittance

To measure the transmittance at MWIR, we fabricated a LC cell using two barium fluoride (BaF_2) substrates. The BaF_2 substrate is transparent from UV to 10μm and its refractive index decreases with wavelength from 1.5 to 1.4 [30]. At λ = 4 μm, the refractive index of BaF_2 is about 1.457. We did not measure the individual refractive indices (n_e and n_o) of M3 in the MWIR region, but based on the E7 data ($n_o \approx 1.50$) [31]we estimated that $n_e \approx 1.77$ and $n_o \approx 1.51$ for M3. To align M3, we spin-coated a thin PI layer on the inner surface of the BaF_2 substrate and gently rubbed the PI layers. Thus, the LC molecules are homogeneously aligned to eliminate light scattering at room temperature. Due to a limited choice of spacers in our lab, we fabricated a LC cell with d = 24μm instead of the targeted 16 μm. The transmittance spectrum was measured by FTIR (Perkin Elmer Spectrum One FTIR Spectrometer) at RT and it is an unpolarized light. Figure 3 shows the measured transmission spectrum. Although there

#226796 - $15.00 USD Received 13 Nov 2014; revised 22 Dec 2014; accepted 22 Dec 2014; published 8 Jan 2015

is a strong absorption peak at λ = 4.45μm due to the CN vibration as expected, its bandwidth is relatively narrow. The baseline transmittance in the off-resonance region is higher than 98%. If we want to study the dichroism of M3, we could simply add an infrared wire grid polarizer in front of the homogeneous-aligned sample cell. Detailed measurement methods and dichroic ratios of some vibration bands of E7, 5CB, and MBBA have been reported in [3, 32].

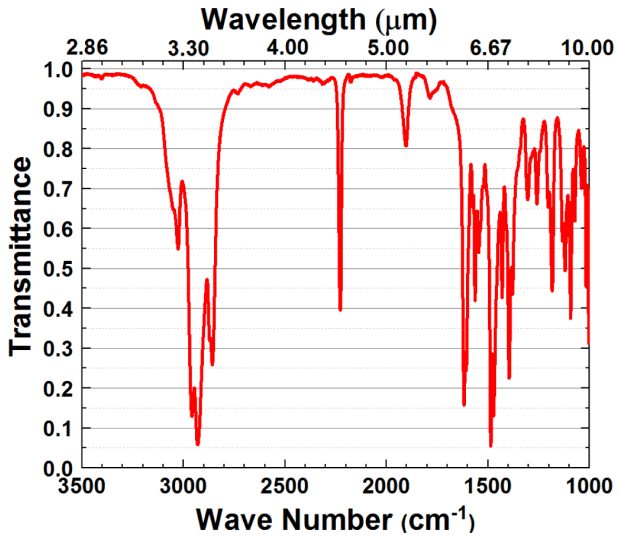

Fig. 3. Measured transmittance spectrum of M3 in the MWIR region with cell gap d = 24μm.

2.3 Dielectric anisotropy

To determine dielectric anisotropy, we measured the capacitance of a homogeneous cell and a homeotropic cell using an HP-4274 multi-frequency LCR meter. For M3, we found $\Delta\varepsilon = 19.6$ at room temperature and 1 kHz. The cyano and chlorine polar groups contribute to this modest dielectric anisotropy.

2.4 Visco-elastic constant

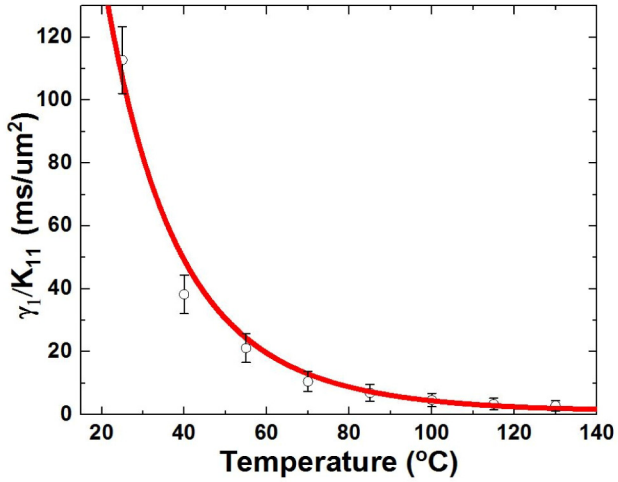

Fig. 4. Temperature dependent visco-elastic coefficients of M3: circles are measured data and red line is fitting with Eq. (6). λ = 633nm.

#226796 - $15.00 USD Received 13 Nov 2014; revised 22 Dec 2014; accepted 22 Dec 2014; published 8 Jan 2015

The visco-elastic coefficient (γ_1/K_{11}) was obtained by measuring the transient free relaxation time for a controlled phase change where δ_0 stands for the total phase change, which needs to be kept small in order to satisfy the small angle approximation:

$$\delta(t) = \delta_0 \exp(-2t/\tau_0), \tag{4}$$

$$\tau_0 = \gamma_1 d^2 / (K_{11}\pi^2), \tag{5}$$

In Eq. (5), τ_0 is the LC director relaxation time, γ_1 is the rotational viscosity, and K_{11} is the splay elastic constant. Figure 4 depicts the temperature dependent visco-elastic coefficient of M3. At room temperature (22°C), γ_1/K_{11} = 113 ms/μm^2. The relatively large visco-elastic constant results from the rigid terphenyl cores, the cyano group and some heavy chlorine substitutions. As the temperature increases, the visco-elastic coefficient decreases dramatically. The solid line in Fig. 4 is theoretical fitting with following equation [33]:

$$\frac{\gamma_1}{K_{11}} = A\frac{\exp(E_a/k_B T)}{(1-T/T_c)^{\beta}}, \tag{6}$$

here A is a proportionality constant, E_a is the activation energy, T is the Kelvin temperature, and k_B is the Boltzmann constant. For M3, we found $A = 4.33\text{x}10^{-6}$ ms/μm^2 and E_a = 432.04 meV. The adjusted R^2 = 0.9957. As expected, such a large viscosity would lead to a slow response time. For instance, if M3 is employed in a reflective-mode LC cell with d = 12 μm, the estimated optical decay time is 830 ms, which is too slow for laser beam steering applications. However, high viscosity is particularly desirable for making polymer network liquid crystal (PNLC) devices with small domain sizes because of its slow diffusion rate, as will be described in detail next.

2.5 PNLC properties

To fabricate PNLCs, we prepared precursors by mixing M3 with monomer RM257 (Merck) and photo-initiator BAPO (Genocure). To obtain different domain sizes, we varied the RM257 concentration from 4 wt% to 6 wt%, while keeping the photo-initiator at 0.5 wt%. Here, we used the mesogenic monomer RM257 to maintain good alignment and obtain spatially uniform phase profile [17]. Next, we filled the precursor into a homogeneous LC cell (ITO glass). The cell gap was 11.8μm and the cell was operated in reflective mode in order to obtain 2π phase change at λ = 4μm and lower operation voltage. A thin cell gap helps to reduce operation voltage [15] because

$$V_{2\pi} \sim \frac{d}{d_1}\sqrt{\frac{K_{11}}{\varepsilon_0 \Delta\varepsilon}}, \tag{7}$$

where d_1 is the average domain size, ε_0 is electric permittivity, and $\Delta\varepsilon$ is dielectric anisotropy. In the UV curing process, we controlled the sample temperature at 0°C to obtain small domain size [18]. Small domain size helps to suppress light scattering (this is particularly important in the visible spectral region) and achieve fast response time, but a trade-off is increased $V_{2\pi}$ as described in Eq. (7). A UV light-emitting diode (LED) lamp (λ = 385nm, intensity = 300 mW/cm^2) was used to cure the precursors and the exposure time was one hour. M3 is a good PNLC host because both the terphenyl core and terminal groups (-CN and -Cl) are UV stable and provide a relatively large viscosity.

For convenience, our PNLC was fabricated on ITO glass substrates, rather than BaF_2. Therefore, we did not measure the MWIR transmittance of PNLC cell directly. However, our PNLC precursors consist of ~95 wt% M3 and ~5% monomer RM257. RM257 is mainly constituted with C-H bonds and phenyl rings, whose vibration bands overlap well with M3.

#226796 - $15.00 USD Received 13 Nov 2014; revised 22 Dec 2014; accepted 22 Dec 2014; published 8 Jan 2015

Therefore, high transmittance at λ = 4-5 μm region should be still maintained in our PNLC device, as Fig. 3 depicts.

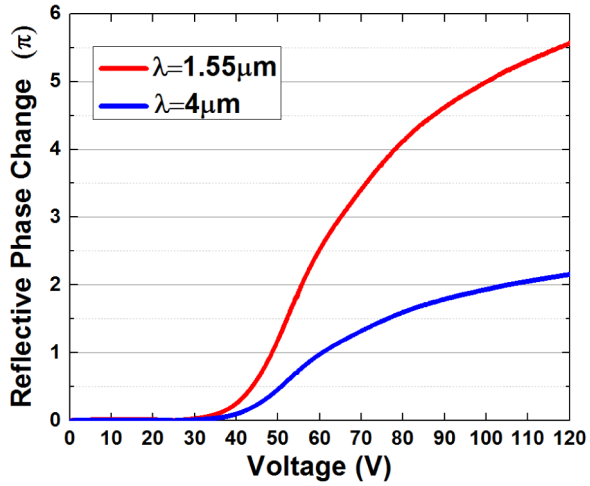

Fig. 5. The voltage-dependence phase change curves of PNLC sample in a reflective mode at λ = 1.55μm and λ = 4μm, respectively. Cell gap d = 11.8 μm.

To characterize the electro-optical properties of our PNLC cells, we measured the *VT* curve at λ = 1.55μm because our ITO glass substrates are not transparent. The transmittance of a 20-nm-thick ITO layer drops to 60% at λ = 4μm [34]. The PNLC cell was sandwiched between two crossed polarizers, with the rubbing direction at 45° to the polarizer's transmission axis. We converted the measured *VT* curve to a voltage-dependent phase (*VP*) curve for each sample. Figure 5 shows the *VP* curve for the PNLC with 5 wt% RM257. According to the dispersion curve shown in Fig. 2, the birefringence is insensitive to the wavelength in the IR region. Therefore, based on Eq. (1) we converted the *VP* curve from λ = 1.55μm to λ = 4μm. To measure the response time of a PNLC, we removed the biased voltage spontaneously at t = 0. The biased voltage was 105V, corresponding to $V_{2\pi}$ at λ = 4μm. The measured phase decay time (from 100% to 10%) fits Eq. (4) well (data not shown here).

Table 2. Operation voltage and decay time of three PNLCs at λ = 4μm and RT.

PNLC	RM257	$V_{2\pi}$ (V)	τ (ms)
1	4%	73	18.0
2	5%	105	3.6
3	6%	>140	1.2

Table 2 lists the $V_{2\pi}$ and response times for the three PNLC samples at λ = 4μm. As the monomer concentration increases from 4 wt% to 6 wt%, $V_{2\pi}$ increases but response time decreases because of the reduced domain size. To balance the operating voltage and response time, we take the PNLC with 5 wt% monomer as an example. The decay time is only 3.6ms, which is ~230X faster than that of the LC host. This fast response time is critically important for the MWIR laser beam steering devices. For MWIR applications, highly transparent substrates and electrodes are required. The thickness of alignment layer is less than 80nm and thus its absorption is negligible. Regarding to substrates, BaF_2 is quite transparent (>95%) from UV to 10μm. For transparent electrodes, we could consider a thin carbon nanotube layer [35], graphene, or meshed metal wires [36].

#226796 - $15.00 USD Received 13 Nov 2014; revised 22 Dec 2014; accepted 22 Dec 2014; published 8 Jan 2015

3. Conclusion

We have developed a terphenyl LC mixture showing high birefringence (Δn = 0.34 at 514nm and Δn = 0.26 at 4μm), good UV stability, and a very broad nematic range (from –40°C to 146.3°C). High birefringence enables a thin cell gap to be used for achieving a 2π phase change at MWIR, while keeping high transmittance (T>98%) and low operation voltage. Although our terphenyl mixture (M3) exhibits a relatively large rotational viscosity, it is highly desirable for making small-domain PNLC because of the slow monomer diffusion rate. Our PNLC devices offer a 2π phase change at λ = 4 μm with fast response time, which is two orders of magnitude faster than that of a nematic LC phase modulator. The operation voltage is around 100V, depending on the monomer concentration. To further reduce operation voltage, two approaches can be considered: larger domain size or an LC host with a larger dielectric anisotropy. The former has a trade-off in slower response time. For the latter, we increase the dipole moments of the compounds listed in Table 1.

Acknowledgment

The authors are indebted to Office of Naval Research for the financial support under contract No. N00014-13-1-0096.

#226796 - $15.00 USD Received 13 Nov 2014; revised 22 Dec 2014; accepted 22 Dec 2014; published 8 Jan 2015